

1 **Narrow-sense heritability estimation of complex traits using identity-by-descent**
2 **information.**

3

4 Luke M. Evans^{1,7}, Rasool Tahmasbi¹, Matthew Jones², Scott I. Vrieze¹, Gonçalo R.
5 Abecasis³, Sayantan Das³, Doug W. Bjelland¹, Teresa R. deCandia¹, Haplotype
6 Reference Consortium, Jian Yang⁴, Michael E. Goddard^{5,6}, Peter M. Visscher⁴, Matthew
7 C. Keller^{1,2,7}

8

9 ¹Institute for Behavioral Genetics, University of Colorado, Boulder, CO 80309

10 ²Department of Psychology and Neuroscience, University of Colorado, Boulder, CO,
11 80309

12 ³Center for Statistical Genetics, Department of Biostatistics, University of Michigan, Ann
13 Arbor, MI 48109

14 ⁴Institute for Molecular Bioscience and the Queensland Brain Institute, University of
15 Queensland, Brisbane, 4072, Queensland, Australia

16 ⁵Faculty of Veterinary and Agricultural Science, University of Melbourne, Parkville,
17 Victoria, Australia

18 ⁶ Biosciences Research, Department of Economic Development, Jobs, Transport and
19 Resources, Victoria, Australia

20 ⁷Corresponding authors luke.m.evans@colorado.edu and matthew.c.keller@gmail.com

21

22 **Running title:** IBD-based heritability estimation

23 **Word count:** 6,964 for main text excluding references, tables, and figures

24 **ABSTRACT**

25 Heritability is a fundamental parameter in genetics. Traditional estimates based
26 on family or twin studies can be biased due to shared environmental or non-additive
27 genetic variance. Alternatively, those based on genotyped or imputed variants typically
28 underestimate narrow-sense heritability contributed by rare or otherwise poorly-tagged
29 causal variants. Identical-by-descent (IBD) segments of the genome share all variants
30 between pairs of chromosomes except new mutations that have arisen since the last
31 common ancestor. Therefore, relating phenotypic similarity to degree of IBD sharing
32 among classically unrelated individuals is an appealing approach to estimating the near
33 full additive genetic variance while avoiding biases that can occur when modeling close
34 relatives. We applied an IBD-based approach (GREML-IBD) to estimate heritability in
35 unrelated individuals using phenotypic simulation with thousands of whole genome
36 sequences across a range of stratification, polygenicity levels, and the minor allele
37 frequencies of causal variants (CVs). IBD-based heritability estimates were unbiased
38 when using unrelated individuals, even for traits with extremely rare CVs, but
39 stratification led to strong biases in IBD-based heritability estimates with poor precision.
40 We used data on two traits in ~120,000 people from the UK Biobank to demonstrate
41 that, depending on the trait and possible confounding environmental effects, GREML-
42 IBD can be applied successfully to very large genetic datasets to infer the contribution
43 of very rare variants lost using other methods. However, we observed apparent biases
44 in this real data that were not predicted from our simulation, suggesting that more work
45 may be required to understand factors that influence IBD-based estimates.

46

47 **KEYWORDS**

48 Identical-by-descent, IBD, heritability, missing heritability, GCTA, shared haplotype

49

50 INTRODUCTION

51 The proportion of phenotypic variance due to additive genetic variation, termed
52 narrow-sense heritability (h^2), is perhaps the most fundamental aspect of a trait's
53 genetic architecture and has both medical and evolutionary significance (Visscher *et al.*,
54 2008; Tenesa and Haley, 2013). Traditionally, h^2 has been estimated from family-based
55 studies (h^2_{FAM}), which have suggested that for many complex traits, much of the
56 phenotypic variance is due to additive genetic variance (Polderman *et al.*, 2015).
57 However, h^2_{FAM} estimates may be biased by factors shared by close relatives, such as
58 non-additive genetic and common environmental effects (Eaves *et al.*, 1978; Coventry
59 and Keller, 2005; Yang *et al.*, 2010; Zuk *et al.*, 2012; Tenesa and Haley, 2013).
60 Alternatively, the variance explained by genetic markers in unrelated individuals, for
61 instance from genome-wide association studies (GWAS), may avoid many of the
62 possible confounding factors of family-based studies. However, the thousands of
63 variants associated with complex traits (Visscher *et al.*, 2012; Ripke *et al.*, 2014; Wood
64 *et al.*, 2014) often explain only a fraction of trait heritability, with the difference often
65 called the “missing heritability.” This missing heritability may result from causal variants
66 (CVs) that are rare or otherwise poorly tagged by commercial genotyping arrays,
67 insufficient sample sizes to detect small effect variants that do not reach genome-wide
68 significance, and biases that inflate h^2_{FAM} .

69 Recently, methods have been developed to estimate the phenotypic variance
70 explained by all genotyped markers simultaneously in unrelated individuals, h^2_{SNP} (Yang
71 *et al.*, 2010; Speed *et al.*, 2012; Bulik-Sullivan *et al.*, 2015). Most of these approaches

72 generally use a genetic relatedness matrix (GRM) that reflects allele sharing or the
73 average correlation between individuals i and j across genotyped SNPs with entries:

$$74 \quad A_{ij} = \frac{1}{m} \sum_k^m \frac{(x_{ik} - 2p_k)(x_{jk} - 2p_k)}{2p_k(1-p_k)} \quad (1)$$

75 where m is the number of SNPs, x_{jk} is the genotype (coded as 0, 1, or 2) of individual j
76 at the k^{th} locus, and p_k is the minor allele frequency (MAF) of the k^{th} locus. The
77 variance-covariance of the phenotype is

$$78 \quad \text{var}(\mathbf{y}) = \mathbf{A}\sigma_v^2 + \mathbf{I}\sigma_e^2 \quad (2)$$

79 where the variance explained by the SNPs (σ_v^2) and error variance (σ_e^2) are estimated
80 using restricted maximum likelihood (REML). The method, termed GREML, is
81 implemented in packages such as GCTA (Yang, *et al.*, 2011). We refer to matrix \mathbf{A} (of
82 dimension $n \times n$ and with elements A_{ij}) as the “SNP-GRM.” The proportion of the
83 variance explained by all SNPs is an estimate of “SNP-based heritability” ($h^2_{SNP} = \sigma_v^2 /$
84 ($\sigma_v^2 + \sigma_e^2$)). By using unrelated individuals, these approaches avoid the confounding of
85 non-additive genetic and environmental effects that can occur in family or twin-based
86 studies, and by estimating all marker effects jointly, the contribution from variants with
87 small effect sizes is captured. Using marker-based approaches, h^2_{SNP} estimates for
88 some complex traits, such as height, have approached h^2_{FAM} , suggesting that little of the
89 heritability remains missing (Yang *et al.*, 2015). For other traits, such as BMI,
90 schizophrenia and neuroticism, h^2_{FAM} estimates remain larger than h^2_{SNP} , and a
91 substantial amount of the heritability remains “still missing” (Lee *et al.*, 2012; Yang *et al.*,
92 2015).

93 Advances on the original approach by Yang *et al.* (2010) have better captured
94 the effects of rare CVs and account for linkage disequilibrium (LD) of markers across

95 the genome, leading to increased h^2_{SNP} estimates (Yang *et al.*, 2015). However, even
96 with the best-performing methods such as MAF- and LD-stratified GREML (GREML-
97 LDMS) and large imputation reference panels, downward bias is likely. Imputation
98 quality declines at low MAF, resulting in a downward bias when causal variants are very
99 rare (MAF<0.0025) and for diverse populations underrepresented in sequencing panels
100 (Evans *et al.*, 2017). The underestimation of variance due to rare CVs may partly
101 explain why h^2_{SNP} remains below h^2_{FAM} for many traits. Thus, developing alternative
102 methods to estimate the variation caused by very rare variants is an important goal.

103 One such alternative is to leverage information on the proportion of the genome
104 shared identical-by-descent (IBD) between pairs of individuals in a sample (Visscher *et*
105 *al.*, 2006; Hayes *et al.*, 2009; Zuk *et al.*, 2012; Browning and Browning, 2013), and use
106 a GRM whose elements are the estimated proportions of IBD between all pairs of
107 individuals (IBD-GRM) to estimate heritability (h^2_{IBD}). This is in some ways similar to
108 classical family-based estimates of heritability, which are based on the expected
109 proportion of the genome shared IBD between close relatives (Falconer and Mackay,
110 1996; Lynch and Walsh, 1998; Visscher *et al.*, 2006). However, rather than using close
111 relatives, an appealing alternative is to estimate pairwise IBD segments directly
112 between all pairs of unrelated (or technically, distantly related) individuals in a sample
113 and use these estimated relationship values to estimate the additive genetic variation.
114 Such an IBD-based approach should capture additive genetic variation due to all but the
115 rarest variants and, so long as close relatives have been removed from the sample, the
116 IBD-based h^2 estimate should be uncontaminated by confounding factors shared by
117 close relatives. Note that we use “IBD” to denote two homologous chromosomal

118 segments that came from the same common ancestor without intervening
119 recombination, such that the sequence identity of the two segments is identical except
120 at sites where new mutations arose since the last common ancestor. The probability
121 that such mutations arose is a function of the time since the last common ancestor, and
122 therefore a function of the length of the shared IBD segment (Wakeley, 2009). Very long
123 segments are therefore more likely to be identical at all sequence sites, whereas shorter
124 ones are more likely to have occasional differences at sites harboring typically very rare
125 variants. Thus, IBD-GRMs calculated from increasingly long IBD thresholds should
126 capture sharing at increasingly rare CVs.

127 Such IBD-based GRMs have been used in several instances to estimate
128 heritability. Price *et al.* (2011) and Zaitlen *et al.* (2013) used IBD segments in an
129 Icelandic dataset with close relatives to estimate heritability in quantitative and disease
130 traits, leveraging the known familial relationships within the Icelandic cohort to identify
131 IBD segments. While they demonstrated that IBD could be used for heritability
132 estimation, using close relatives leads to possible confounding of shared environmental
133 or non-additive genetic effects, as noted above. Indeed, Zaitlen *et al.* (2013) found
134 higher heritability estimates using closer relatives, consistent with confounding from
135 non-additive genetic and/or shared environment effects. Using simulated data, Zuk *et al.*
136 (2012) demonstrated that the slope estimated from regressing phenotypic similarity
137 (defined as the standardized phenotypic product of individuals i and j , $Z_i \times Z_j$) on the
138 IBD-GRM elements from long IBD segments—known as Haseman-Elston (H-E)
139 regression—provides an unbiased estimate of the additive genetic variance in isolated
140 founder populations. Browning and Browning (2013) estimated IBD tracts in a Finnish

141 cohort of 5,400 individuals, and used the resulting IBD GRM in both H-E regression and
142 GREML to estimate h^2_{IBD} for nine quantitative metabolic traits. h^2_{IBD} was higher than
143 h^2_{SNP} for only five of the nine traits, and never significantly so. The most notable result of
144 their study was the over two-fold higher standard errors for h^2_{IBD} (~ 0.17) compared to
145 h^2_{SNP} (~ 0.07), due to the lower variation in the off-diagonal elements of the IBD-GRM
146 compared to the SNP-GRM, suggesting that very large sample sizes will be required to
147 obtain meaningful results in non-founder populations.

148 Several important questions about IBD-based heritability estimation remain in
149 light of these findings. First, can an IBD-based approach account for very rare CVs?
150 Previous studies (e.g., Browning and Browning, 2013) have simulated CVs from SNPs
151 present on genotyping arrays, which are more common, have generally higher LD than
152 most variants throughout the genome, and are shared across ancestry groups, and
153 therefore do not provide an accurate picture of how h^2 estimation methods perform
154 when CVs do not share these same properties. Thus, it is unclear whether h^2_{IBD}
155 estimates are unbiased estimates of h^2 in the presence of rare CVs. Second, the
156 studies mentioned above utilized isolated founder populations that were both more
157 homogeneous and more related than non-founder populations. To what extent does
158 genetic stratification bias h^2_{IBD} , and how feasible are such IBD-based method in
159 samples from non-founder populations, which are much more readily available?

160 To address these questions, we used thousands of recently sequenced whole
161 genomes from the Haplotype Reference Consortium (McCarthy *et al.*, 2016) to simulate
162 phenotypes under a range of conditions, including various genetic architectures and
163 levels of stratification, then estimated narrow-sense heritability (h^2_{IBD}) using the an IBD-

164 GRM, either alone or in combination with various SNP-based GRMs. By simulating CVs
165 from whole genome sequences rather than commercial array SNPs, our study was able
166 to examine the role of all but the rarest frequency classes of CVs in the genome under
167 realistic genomic conditions. We then estimated h^2_{IBD} for height and BMI in the UK
168 Biobank with over 120,000 individuals.

169

170 **MATERIALS AND METHODS**

171 *Samples and Population Structure*

172 We tested the h^2_{IBD} estimation method using simulated phenotypes derived from
173 Haplotype Reference Consortium (HRC) whole genome sequence data (McCarthy *et*
174 *al.*, 2016). Full details of the HRC can be found in McCarthy *et al.* (2016). Briefly, this
175 resource comprises roughly 32,500 individual whole genome sequences from multiple
176 sequencing studies, with phased genotypes with a minor allele count of at least 5 at all
177 sites. This large sequence dataset allowed us to simulate CVs across all MAF classes
178 down to $\sim .0003$ with real patterns of LD (within and among chromosomes). It also
179 allowed us to simulate SNP markers available on existing commercial genotyping arrays
180 in order to mimic the process of IBD detection in SNP data. We obtained permission to
181 access the following HRC cohorts (recruitment region & sample size): AMD (Europe &
182 worldwide; 3,189), BIPOLAR (European ancestry; 2,487), GECCO (European ancestry;
183 1,112), GOT2D (Europe, 2,709), HUNT (Norway; 1,023), SARDINIA (Sardinia; 3,445),
184 TWINS (Minnesota; 1,325), 1000 Genomes (worldwide; 2,495), UK10K (UK; 3,715)
185 (see (McCarthy *et al.*, 2016) for additional details of the HRC). This set of cohorts, which
186 included isolated subpopulations of European descent, allowed investigation into the

187 effects of stratification on estimates. The subset totaled 21,500 whole genome
188 sequences comprising 38,913,048 biallelic SNPs. This is the same set of individuals
189 and simulated phenotypes used in Evans *et al.* (2017) to compare SNP-based
190 heritability methods. Below, we briefly describe our approach.

191 Our goal was to assess the accuracy and potential bias of the h^2_{IBD} estimation
192 method using data similar to those collected for a typical GWAS analysis and h^2_{SNP}
193 estimation. In order to mimic this kind of data, we first extracted variant positions
194 corresponding to a widely-used commercially available genotyping array, the UK
195 Biobank Affymetrix Axiom array. We then identified individuals of primarily European
196 ancestry, using principal components analysis with 133,603 MAF- and LD-pruned
197 markers (plink2 (Chang *et al.*, 2015) command: --maf 0.05 --indep-pairwise 1000 400
198 0.2) to identify a grouping associated with the 1000 Genomes European individuals in
199 the HRC. This dataset comprised 19,478 individuals including Finnish and Sardinian
200 samples (Fig. S1).

201 From within this European ancestry dataset, we identified clusters that contained
202 different levels of genetic heterogeneity within them (Fig. S2). The most structured
203 group contained all samples (N=19,478). The somewhat structured group excluded
204 Sardinian and Finnish samples (N=14,424). The low structure group contained
205 northern/western European samples (N=11,243), and the least structured was a subset
206 of mainly British Isles samples (N=8,506). We used GCTA (Yang, *et al.*, 2011) with LD-
207 and MAF-pruned SNPs to estimate relatedness and remove the minimal number of
208 individuals from pairs with relatedness > 0.1 within each of the four samples. In the most
209 homogeneous and smallest sample with no genetic structure, this left 8,201 individuals.

210 In order to eliminate the influence of varying sample size in our comparison across the
211 range of stratification, we randomly chose 8,201 of the unrelated individuals from within
212 each of the other three stratification subsamples. We similarly tested a lower
213 relatedness cutoff of 0.05 within each group (leaving 7,792; 8,115; 8,129; and 8,186
214 individuals for the four subsamples), and used both subsets later to examine how a 0.1
215 or 0.05 relatedness cutoff influences h^2_{IBD} estimates.

216

217 *Simulated Phenotypes Using Whole Genome Sequencing Data*

218 To test how h^2_{IBD} estimation our method performed on a range of genetic
219 architectures, we simulated phenotypes from CVs drawn randomly from five MAF
220 ranges: common (MAF>0.05), uncommon (0.01<MAF<0.05), rare (0.0025<MAF<0.01),
221 very rare (0.0003<MAF<0.0025), and all variants randomly drawn with MAF>0.0003.
222 Phenotypes were generated with 1,000 or 10,000 CVs from the model $y_i = g_i + e_i$, where
223 $g_i = \sum w_{ik}\beta_k$, w_{ik} is the genotype (coded as 0, 1, or 2) of individual i at the k^{th} CV, and β_k
224 is the k^{th} allelic effect size, drawn from $\sim N(0, 1/[2p_k(1-p_k)])$, where p_k is the MAF of allele
225 k within each of the four samples, which assumes larger additive effects for rarer
226 variants. The g_i 's were standardized and residual error was added as $\sim N(0, (1-h^2)/h^2)$ for
227 a simulated h^2 of 0.5. A total of 400 replications were performed for each CV MAF range
228 and for each of the four stratification subsets.

229

230 *Mixed Models for Heritability Estimation*

231 We estimated heritability for each simulation using GCTA (Yang, Lee, *et al.*,
232 2011). We tested different models to assess our IBD-based GREML method (GREML-

233 IBD). First, we used the single IBD-GRM with GREML to estimate h^2_{IBD} . Second, to
234 partition the genetic variance into that tagged by common SNPs and that tagged by
235 haplotype sharing, presumably from rarer CVs, we used a two GRM model (GREML-
236 IBD+SNPs) with the IBD-GRM (h^2_{IBD}) and a common SNP-GRM derived from Axiom
237 array positions with $MAF > 0.01$ (h^2_{SNP}). Last, we estimated genetic variances due to LD-
238 and MAF-stratified imputed variant SNP-GRMs (h^2_{SNP}) as well as the IBD-GRM (h^2_{IBD})
239 as a comparison to the GREML-LDMS method, which we term GREML-IBD+LDMS.
240 From previous work, we knew that GREML-LDMS underestimates variance attributable
241 to the rarest CVs when using imputed data. We therefore wished to determine if the
242 IBD-GRM could capture that missing heritability. To do this, we estimated 16 SNP-
243 GRMs stratified into the above 4 MAF categories and 4 LD score quartiles using
244 imputed genome-wide variants, and included these plus the IBD GRM in the model (17
245 GRMs total). To determine if the IBD-GRM captured the genetic variance due to the
246 rarest CVs, we also tested a model with 12 SNP-GRMs, removing the rarest MAF
247 category described above, for a total of 13 GRMs in the analysis (three MAF categories
248 X four LD score quartiles + 1 IBD-GRM). To impute, we first phased SNP data using
249 SHAPEIT2 (Delaneau *et al.*, 2013), imputed using minimac3 (Das *et al.*, 2016), and
250 retained variants with imputation $R^2 \geq 0.3$ (Yang *et al.*, 2015). We used the HRC
251 sequence data as our imputation reference panel after removing all target (8201
252 unrelated + relatives) individuals in the HRC reference panel, thereby assuring
253 ~independence (no relatedness) between the target and reference panels. Additional
254 details of the imputation procedure can be found in Evans *et al.* (2017). We estimated
255 LD scores for the LD stratification using GCTA. In all cases we used the `-reml-no-`

256 constrain option of GCTA, and included 20 principal components (PCs; 10 from
257 worldwide PC analysis and 10 from the specific subsample PC analysis) as continuous
258 covariates, with sequencing cohort as a categorical covariate.

259

260 *Estimating IBD-GRMs*

261 To mimic computationally phased SNP data with realistic phase errors, we first
262 un-phased the sequence data for each data subset and then re-phased the Axiom array
263 positions using SHAPEIT2 (Delaneau *et al.*, 2013). We then used FISHR2 (Bjelland *et*
264 *al.*, 2017) to identify shared haplotype segments that are putatively IBD across all pairs
265 of individuals within each of our four structure samples. FISHR2 first uses a modified
266 version of GERMLINE (Gusev *et al.*, 2009) to find candidate IBD segments. It then
267 improves the accuracy of the segment endpoints by comparing an observed moving
268 average of haplotype mismatches (potential phase or SNP call errors) for a given
269 candidate IBD segment to (a) the distribution of haplotype mismatches in segments that
270 are almost certainly IBD (the middlemost sections of very long IBD segments) and (b)
271 the distribution of haplotype mismatches in segments that are almost certainly non-IBD
272 (between random pairs of individuals at matched locations). FISHR2 truncates
273 candidate segments when this moving average becomes more consistent with non-IBD
274 than IBD. FISHR2 is more accurate than leading competitors at detecting long (> 3 cM)
275 IBD segments and is the only software that gives unbiased estimates of the true length
276 of IBD segments. The parameters we used for FISHR2 were stringent (command line -
277 err_hom 4 -err_het 1 -min_snp 128 -min_cm_initial 1 -min_cm_final 1 -window 50 -
278 gap 100 -h_extend -w_extend -homoz -emp_ma-threshold 0.06 -emp-pie-threshold

279 0.015 -count.gap.errors TRUE), chosen to minimize false positive IBD detection
280 (Bjelland *et al.*, 2017). We used an initial length threshold of 1 cM, but because longer
281 IBD segments are more likely to share rare variants, we also identified segments of
282 length greater than 2, 3, 4, 6, 9, and 12 cM. The FISHR2 parameters we used should
283 lead to consistently low false positive rates (<.05) at all threshold lengths, and should
284 lead to a sensitivity that increases as a function of the length of the true IBD segments,
285 and should be >.90 for IBD segments >3cM (Bjelland *et al.*, 2017). To reduce the
286 influence of low recombination regions artificially extending segments (e.g., due to one
287 or a few matching IBS SNPs that are far from the termini of true IBD segments), we
288 windsorized genetic map positions by setting the maximum distance between adjacent
289 markers to 0.2 cM, and used an initial 1 cM minimum IBD segment length threshold.

290 We then summed the length in Mb of all segments shared between each pair of
291 individuals and divided by twice the length of the genome. This IBD-GRM then
292 represents the estimated proportion of the genome, D_{ij} , shared IBD between individuals
293 i and j in the sample, similar to the A_{ij} elements of the SNP-GRM. We created IBD-
294 GRMs for each minimum segment cM length threshold. As recombination rate varies
295 throughout the genome, in two of the subsamples we also tested whether an IBD-GRM
296 based on the summed cM length of segments influences heritability estimates.

297

298 *Stratification Effects*

299 We performed four additional analyses to further determine the influence of
300 stratification on h^2_{IBD} estimates. First, to test whether bias observed in stratified samples
301 was due to inadequate control of structure, we ran K-means clustering on the somewhat

302 stratified subsample for K=2 clusters, then ran PC analysis within each of the two
303 clusters. We included the first 35 PCs within each cluster, for a total of 90 PCs (the
304 original 20 plus 35 from each cluster). Because PC analysis was run within each cluster
305 separately, we set the PC scores for the alternate cluster to 0 (the mean).

306 Second, we tested, within the stratified subsample, whether including 10
307 additional PCs from very rare variants could correct for the upward bias (Mathieson and
308 McVean, 2012). We used 150,000 randomly selected very rare SNPs from the WGS
309 data and pruned for LD (plink2 command: --indep-pairwise 1000 400 0.2), leaving
310 129,710 variants for the PCA. As a comparison, we also estimated heritability with no
311 covariates included.

312 Third, we estimated h^2_{IBD} for phenotypes in which all CVs were drawn from odd
313 chromosomes using IBD-GRMs estimated only from the even chromosomes. The
314 presence of uncontrolled cryptic relatedness or population structure can lead to cross-
315 chromosome LD that inflates h^2 estimates (Yang *et al.*, 2011). We estimated the
316 correlation of off-diagonal GRM elements between the IBD-GRMs from even
317 chromosomes and those from odd chromosomes. We also examined the correlation
318 between the off-diagonal elements from IBD-GRMs and the off-diagonal elements from
319 GRMs built from very rare ($0.0003 < \text{MAF} < 0.0025$) and common ($\text{MAF} > 0.05$) sequence
320 variants. This tested whether correlations between even and odd chromosome IBD-
321 GRMs were stronger in more stratified subsamples, and whether the correlation with
322 very rare variants was stronger with increasing minimum cM length of the IBD-GRM.

323 Last, simultaneously fitting GRMs derived from each chromosome protects
324 against cross chromosome correlations induced by stratification or cryptic relatedness

325 because the estimates of variance explained by one GRM are conditional on the other
326 GRMs (Yang *et al.*, 2011). However, because the variances of the off-diagonal
327 elements in the IBD-GRMs were so small, models with 22 IBD-GRMs would not
328 converge. Instead, we tested a two GRM model with one IBD-GRM estimated from the
329 odd numbered chromosomes and a second from the even numbered chromosomes,
330 which should partially address the effects of long-range LD (Speed *et al.*, 2012).

331

332 *Heritability of Complex Traits in the UK Biobank*

333 We applied the IBD-based approaches to height and body mass index (BMI) data
334 in the UK Biobank, a very large resource of ~500K adults from the UK, genotyped using
335 the Affymetrix Axiom array (Sudlow *et al.*, 2015). The current release includes ~150K
336 genotyped individuals, imputed using the combined UK10K/1000 Genomes reference
337 panels. We used this resource previously, and full details on quality control can be
338 found in Evans *et al.* (2017). We identified putative IBD segments as described above
339 using FISHR2 and then calculating IBD-GRMs with minimum cM thresholds of 2, 3, 4, 6,
340 9, and 12cM. We applied a relatedness cutoff of 0.05, and used individuals of European
341 ancestry, resulting in a final sample size of ~120K individuals included in the analysis
342 (Fig. S2). We used GCTA to estimate variance components and included sex, UK
343 Biobank assessment centre, genotype measurement batch, and qualification (highest
344 level of educational attainment) as categorical covariates, and the Townsend
345 deprivation index, age at assessment, age at assessment squared, and the 15 PC
346 scores from the UK Biobank as quantitative covariates. We compared these models
347 using Akaike information criterion with sample size correction (AICc) (Burnham and

348 Anderson, 2002), and used this to determine if additional information was added by
349 using an IBD-GRM.

350

351 **RESULTS**

352 *Simulated Phenotypes – GREML-IBD*

353 Using a single IBD-GRM, h^2_{IBD} estimates varied greatly depending on the MAF
354 range of the CVs in simulated phenotypes and the amount of stratification in the
355 subsample (Fig. 1). In the two more homogeneous subsamples, h^2_{IBD} increased then
356 stabilized with increasing IBD segment length threshold. The 95% CI overlapped the
357 true heritability (0.5) for all IBD thresholds > 4 cM and for all CV MAF classes,
358 suggesting that GREML-IBD produces unbiased estimates of h^2 in relatively
359 homogeneous samples. For phenotypes simulated from common CVs, unbiased
360 estimates of h^2_{IBD} were also obtained using shorter cM thresholds. Results were similar
361 for different relatedness thresholds (Figs S3 & S4) and for larger numbers of CVs (Fig.
362 S5), although h^2_{IBD} appeared to be biased upwards in phenotypes with 10,000 common
363 CVs and long IBD length thresholds in the low stratification subsample (Fig. S5).

364 In the two most stratified samples, we observed upward biases at long cM IBD
365 thresholds, particularly for the rarest CVs ($h^2_{IBD} > 1$). This bias remained when using
366 higher or lower relatedness thresholds (Figs. S3-4), and with 10,000 CVs (Fig S5).
367 Controlling for 70 additional PCs or with additional PCs from very rare variants did not
368 correct for the upward bias in very rare CV phenotypes, though inclusion of PCs did
369 correct for bias in common CV phenotypes (Fig. S6). Furthermore, this bias was not
370 mitigated by summing genetic length (cM) of IBD segments for calculating the GRM

371 rather than physical length (Fig. S7) nor when using a two-GRM model, with one IBD-
372 GRM calculated from even-numbered chromosomes and the second from odd-
373 numbered chromosomes (Fig. S8-S9). Fitting a larger number of IBD-GRMs (e.g., one
374 per chromosome) would better capture all the long-range correlations and might better
375 mitigate the bias, but this approach is impractical for GREML-IBD in real data because
376 the low variance of D_{ij} creates estimation problems. Thus, stratification has strong
377 impacts on GREML-IBD estimates of heritability that we were unable to control for.

378 To explore why stratification had such strong influences on h^2_{IBD} , we first
379 examined the correlations of off-diagonal GRM elements between the odd chromosome
380 GRMs and even chromosome GRMs. Stratification clearly led to stronger long-range
381 correlations, as did, in most subsamples, longer IBD thresholds for the GRM (Fig. S10).
382 In the two least stratified subsamples, the correlation of even chromosome IBD-GRMs
383 with odd chromosome WGS SNP-GRMs, estimated from either common or very rare
384 WGS variants, was weak, and did not change drastically with increasing cM thresholds.
385 There were stronger correlations overall in the two most stratified subsamples,
386 especially between even chromosome IBD-GRMs and odd chromosome GRMs built
387 from either IBD segments or from very rare WGS variants. Thus, stratification induced
388 long-range correlations, such that D_{ij} for a pair of individuals at one chromosome
389 predicted rare variant sharing at other chromosomes, which can presumably lead to
390 over-estimation of h^2_{IBD} due to rare CVs being redundantly tagged by IBD sharing.

391 In simulations with odd chromosome CVs and IBD-GRMs calculated from even
392 chromosomes only, we observed upward biases in h^2_{IBD} estimates for long IBD
393 thresholds that were particularly severe in stratified samples with rare odd-chromosome

394 CVs (Fig. S11). This pattern of results was similar to the pattern observed in our primary
395 simulations (Fig. 1), consistent with the explanation that the upward biases in h^2_{IBD} for
396 rare CVs we observed at long IBD thresholds was due to long-range, redundant tagging
397 of CVs in stratified samples. Note that the simulated h^2 for the even chromosomes was
398 0. Because there is more recent common ancestry within than between subpopulations,
399 there is more sharing of long IBD segments—and importantly more sharing of rare
400 (recently arisen) causal variants. Consequently, due to stratification, long, shared IBD
401 segments at one genomic location weakly predict not only sharing of long IBD
402 segments, but also sharing of rare variants and shorter IBD segments, at other genomic
403 locations. This redundant tagging of rare causal variants across the genome in stratified
404 samples presumably leads to inflated h^2_{IBD} estimates. The same phenomenon has been
405 described h^2_{SNP} in the context of stratification (Yang *et al.*, 2011; Speed *et al.*, 2012),
406 although the bias is less extreme and, because the variance of A_{ij} elements is much
407 greater than the variance of D_{ij} , is more easily alleviated by fitting multiple GRM models.
408

409 *Simulated Phenotypes – GREML-SNPs+IBD*

410 The second model we tested was GREML-SNPs+IBD, which included a common
411 SNP-GRM and the IBD-GRM. For phenotypes with 1,000 or 10,000 CVs, the total
412 heritability ($h^2_{IBD}+h^2_{SNP}=h^2_{Total}$) was unbiased in the two least stratified subsamples
413 regardless of the CV MAF range (Fig. S12, S13). However, h^2_{Total} was again
414 increasingly over-estimated in the two most stratified samples for very rare CV
415 phenotypes. As expected, partitioning the variance to each of the GRMs, GREML-
416 SNPs+IBD attributed more of the phenotypic variance to the common SNP-GRM when

417 the CVs were common, and more of the variance to the IBD-GRM when the CVs were
418 rarer (Figs. S14-S15). For common CV phenotypes, the variance attributable to the
419 common SNP-GRM was overestimated by ~20%, which is consistent with previous
420 findings for a common SNP-GRM based on the Axiom array positions and occurs
421 because CVs in the common bin have higher average MAF than the SNPs on the
422 Axiom array (Evans *et al.*, 2017). Interestingly, this overestimate was balanced by a
423 negative variance estimate attributed to the IBD-GRM, such that the total estimated
424 heritability was unbiased at ~0.5 (Figs. S12-S15). Nevertheless, h^2_{IBD} continued to be
425 overestimated for very rare CV phenotypes in structured samples.

426

427 *Simulated Phenotypes – GREML-LDMS+IBD*

428 Our third model included 16 imputed variant GRMs that were MAF- and LD-
429 stratified, and the IBD-GRM. We found that across subsamples, GREML-LDMS+IBD
430 produced unbiased h^2_{Total} estimates with either 1,000 CVs or 10,000 CVs across all CV
431 MAF ranges (Figs. S16-S17). Partitioning the variance among GRMs revealed that for
432 the rare and very rare CV phenotypes, the IBD-GRM explained a small amount of the
433 variance, but was near-zero otherwise (Figs. S18-S19).

434 When we excluded the rarest MAF bin from the model, leaving 12 imputed
435 variant GRMs plus the IBD-GRM, GREML-LDMS+IBD produced unbiased h^2_{Total}
436 estimates with either 1,000 CVs or 10,000 CVs across all CV MAF ranges in
437 subsamples with little or no stratification (Figs. 2, S20). However, with increased
438 stratification, h^2_{Total} estimates were again overestimated for very rare CV phenotypes in
439 the context of stratification. Partitioning the variance into that attributable to the LDMS

440 imputed-variant GRMs and the IBD-GRM showed that, in unstratified samples, most of
441 the genetic variance was attributable to the LDMS GRMs for CV MAF ranges > 0.0025
442 while the IBD-GRM captured the genetic variance for very rare CV MAF ranges
443 ($0.0003-0.0025$) (Figs. 3, S21). While the variance attributed to the LDMS GRMs was
444 never overestimated, that attributed to the IBD-GRMs at longer IBD thresholds was
445 overestimated, resulting in total heritability estimates > 1 for the rarest CV phenotypes in
446 the presence of stratification.

447

448 *Real Phenotypes from the UK Biobank*

449 Using GREML-IBD, h^2_{IBD} for height (but not for BMI) increased with longer
450 minimum shared haplotype length, did not stabilize at longer segment thresholds, and
451 appeared upwardly biased, similar to what we observed in stratified samples in our
452 simulations (Fig. 4a, Table S1). The 95% CIs increased with longer minimum IBD
453 length, as expected given the lower variance in D_{ij} at longer segment thresholds. For
454 comparison, h^2_{SNP} estimates from approaches using only SNPs are also presented in
455 Table S1.

456 Using either GREML-SNPs+IBD or GREML-LDMS+IBD, we found similar
457 patterns of increasing h^2_{IBD} estimates with longer minimum IBD length for height, but the
458 pattern was less extreme, and 95% CIs were generally smaller (Fig. 4b, Table S1).
459 Results for GREML-LDMS+IBD either including the rarest MAF category or excluding it
460 were similar: height h^2_{IBD} estimates increased from 0.75 to 1.1 across the range of
461 minimum IBD lengths we examined. This increase in h^2_{IBD} was due to increasing
462 estimates of variance attributable to the IBD-GRM rather than to the imputed variant

463 SNP-GRMs (Fig. S22, Table S1). BMI h^2_{IBD} estimates were again ~ 0.2 - 0.3 , though at
464 longer minimum IBD length thresholds the standard errors were large, and the 95% CI
465 overlapped 0 (Table S1).

466 Interestingly, inclusion of the IBD-GRM in addition to the SNP-GRM or LDMS-
467 GRMs often improved model fit and resulted in a lower AICc (Table S1). Often the
468 lowest AICc was found with shorter IBD minimum length thresholds. For instance, for
469 height, the minimum AICc was found when using all LD- and MAF-stratified imputed
470 variant GRMs and the IBD-GRM with a 3cM minimum IBD length threshold (Table S1),
471 while AICc increased with longer length thresholds. Thus, while increasing the minimum
472 length threshold led to unreasonable and uninterpretable total heritability estimates, at
473 shorter IBD length thresholds, the inclusion of the IBD-GRM was preferred. This
474 indicates that some additional variance remains to be explained over using only
475 imputed-variant GREML-LDMS and that inclusion of the IBD-GRM led to models that
476 better explained the observed phenotypic similarity, perhaps reflecting the effect of CVs
477 that are not well captured by imputed variants.

478

479 **DISCUSSION**

480 We present here the most thorough assessment to-date of an IBD-based
481 heritability estimation approach. The interest in using IBD information in classically
482 unrelated samples to estimate heritability arises from the potential to estimate the full
483 narrow-sense heritability without the confounding of effects shared within families that
484 can bias estimates when close relatives are used, and without the downward bias in
485 estimation when CVs are rare or poorly tagged by SNPs. We demonstrated that

486 GREML-IBD can produce unbiased heritability estimates in realistic whole-genome SNP
487 data so long as there is little genetic stratification in the sample. Moreover, although we
488 showed only marginal improvement, at best, over imputed variant-based approaches,
489 IBD-based approaches should do increasingly better than ones based on imputed SNPs
490 in estimating heritability if CVs are even rarer ($MAF < .0003$) than we could simulate
491 here. That said, no estimation based on genomic sharing can capture variation due to
492 CVs that occur only once in the sample.

493 While IBD-based approaches are appealing in principle, our study highlights two
494 important drawbacks. First, stratification can bias heritability estimates upward,
495 depending on the allele frequencies of CVs. The effect of stratification is strong when
496 CVs are very rare, and is not controlled by inclusion of a large number of PC covariates,
497 the typical approach to controlling such effects (Price *et al.*, 2010), or even PCs derived
498 from very rare variants (Mathieson and McVean, 2012). Similar overestimates have
499 been observed in a related method that used sharing at predefined, segregating
500 haplotypes (Bhatia *et al.*, 2016). Overestimates appear to stem from redundant tagging
501 by long IBD segments of very rare CVs as well as shorter IBD segments, particularly in
502 stratified samples. Previous studies using IBD-based approaches (Zuk *et al.*, 2012;
503 Browning and Browning, 2013) used isolated, homogeneous populations, which should
504 mitigate this source of bias. Our simulation results suggest somewhat less homogenous
505 samples, such as those of general northern/western European ancestry, can be used to
506 derive unbiased heritability estimates so long as there are no additional confounding
507 factors.

508 Second, the standard error (SE) of the h^2_{IBD} estimate is large due to the very low
509 variance in IBD sharing among unrelated individuals in large, non-founder populations.
510 For example, for height in the UK Biobank when using GREML-LDMS+IBD, total
511 heritability $SE \geq 0.053$ for minimum IBD lengths ≥ 6 cM, largely due to the IBD-GRM
512 variance component SE. However, using just the imputed variant GREML-LDMS
513 approach $SE=0.015$. Thus, while the GREML-LDMS+IBD may have accounted for more
514 of the genetic variance, it did so with substantially lower precision. Very large sample
515 sizes will be required to reach high levels of precision. Taken together, it is not clear
516 whether the increased variance explained, arising from capturing rare CVs with IBD-
517 based GRMs, outweighs the very large increase in standard errors and the increased
518 potential for bias due to stratification or other factors we did not model here.

519

520 *Heritability of Real Complex Traits*

521 Our results from real UK Biobank data for height demonstrate the potential for
522 additional biases of an IBD-based approach that were not captured in our simulation.
523 The estimates of total heritability for height increased with minimum IBD cM length, and
524 were much greater than other reported estimates (e.g., Yang *et al.*, 2015; Evans *et al.*,
525 2017). This was unexpected given that the UK Biobank sample was similar to simulated
526 data with respect to stratification. It is possible that the CVs, particularly rare CVs,
527 underlying height are more geographically stratified than those that influence BMI.
528 Indeed, evidence suggests that across Europe, genetic variance in height is more
529 geographically structured than BMI, though both traits are more genetically structured
530 than a neutral, drift-only model (Robinson *et al.*, 2015). However, environmental

531 variation in BMI across Europe appears to be stronger than genetic differentiation
532 (Robinson *et al.*, 2015). Thus, for height, neutral structure (shared long IBD segments)
533 may covary with geographical variation in the CVs themselves, and lead to inflation of
534 h^2_{IBD} . While consistent with our observed likely upward bias in height h^2_{IBD} but not BMI
535 h^2_{IBD} , we cannot be certain that divergent selection is driving these patterns.

536 Vertically-transmitted non-genetic effects, shared common environmental effects,
537 and assortative mating may also confound estimates of h^2_{IBD} . Estimates of h^2_{FAM} using
538 close relatives can be altered by these factors (Eaves *et al.*, 1978; Martin *et al.*, 1978;
539 Coventry and Keller, 2005; Zuk *et al.*, 2012). It is currently unknown how GREML-based
540 estimates, and IBD-based approaches in particular, are affected by assortative mating.
541 Common environmental effects, which can induce similarity across highly extended
542 pedigrees, would be confounded with IBD sharing, and are therefore a potential source
543 of bias in IBD-based estimates. Such extended pedigree environmental similarity would
544 be difficult to simulate using our simulation method, and so we did not explore how such
545 an effect might bias h^2_{IBD} . Our results in the UK Biobank data suggest that our
546 assumption that removing close relatives (relatedness < 0.05) would mitigate shared
547 environment confounding may require further investigation. The use of lower
548 relatedness thresholds may alleviate the problem, but lower relatedness thresholds
549 decrease the sample size and variance of IBD sharing and therefore further exacerbate
550 the already high standard errors of these estimates. Rare variants are more differentially
551 confounded by stratification than common variants, and typical approaches using PCA
552 may not fully correct for such confounding (Mathieson and McVean, 2012). Extremely
553 rare SNPs, as with long IBD segments, will co-segregate along extended pedigrees,

554 and future work must focus on the role of confounding between familial and
555 environmental effects and rare variants or long IBD segments.

556 While we cannot conclude with certainty which factors led to the apparent bias in
557 height h^2_{IBD} , estimates of h^2_{IBD} for BMI were more stable and also in line with previous
558 reports. They suggest that BMI h^2 is roughly 0.25-0.3, with up to 5% of the total
559 phenotypic variance due to very rare or otherwise poorly-imputed variants that are
560 captured by the IBD-GRM (see Table S1). As estimates from classical twin design
561 studies range from 0.4-0.8, this suggests that much of the family-based estimates are
562 due to shared environment, assortative mating, or non-additive genetic variance,
563 supported by extended twin design variance estimates (Coventry and Keller, 2005;
564 Keller and Coventry, 2005). This also suggests that little unexplained variance remains
565 for BMI, as estimates of BMI h^2_{SNP} from recent studies range from 0.21 (Locke *et al.*,
566 2015) to 0.27 (Yang *et al.*, 2015).

567 Our findings may also offer context to the observed heritability estimates reported
568 by several other studies that used haplotype-based approaches. Browning and
569 Browning (2013) reported h^2_{IBD} for BMI of 0, with standard error of 0.16 (height was not
570 measured), although their upper 95% CI estimate is not inconsistent with a true h^2 of
571 0.25-0.3. This low estimate may simply be due to sampling variance, arising from the
572 small number of individuals (5,402) in the Finnish sample they used. Zaitlen *et al.*
573 (2013) used IBD among close relatives to derive estimates of h^2_{IBD} of 0.69 for height
574 and 0.42 for BMI. As discussed by the authors, these estimates may be upwardly
575 biased due to common environmental and non-additive genetic effects.
576

577 *Conclusions*

578 Identical-by-descent haplotypes in common between a pair of chromosomes
579 capture sharing at all variants that existed along their length in the last common
580 ancestor. The ability to estimate such IBD segments using SNP data means that there
581 is potential to estimate narrow-sense heritability of traits in a way that should be
582 unbiased by factors that bias SNP or family-based estimates. We conclude that IBD-
583 based estimates can be used to obtain estimates of the near full narrow-sense
584 heritability. However, IBD-based estimates are imprecise and very sensitive to
585 stratification. Moreover, when we estimated h^2_{IBD} in real data, we observed unexpected
586 biases that appeared similar to those that we had observed in more stratified samples in
587 our simulation, which suggests that there are biases in real data that we were not able
588 to adequately capture in our simulation. Taken together, these factors diminish the
589 appeal of IBD-based approaches for estimating heritability, especially when compared
590 to approaches that use imputed variants, such as GREML-LDMS. Nevertheless, until
591 whole genome sequence data is feasible for the large sample sizes required for h^2
592 estimation from genotype data, IBD-based estimates may be able to capture the rarest
593 CVs better than imputation. In particular, though larger and more diverse reference
594 panels are becoming available, isolated populations may not be well-represented. IBD-
595 based approaches offer a method to capture rare genome-wide variants not
596 represented in imputation reference panels, and these isolated, homogeneous
597 populations may also be the most advantageous for IBD-based heritability estimation
598 due to the larger variance in IBD sharing.
599

600 **ACKNOWLEDGEMENTS**

601 This work utilized the Janus supercomputer, which is supported by the National Science
602 Foundation (award number CNS-0821794), the University of Colorado Boulder, the
603 University of Colorado Denver, and the National Center for Atmospheric Research, and
604 is operated by the University of Colorado Boulder. We thank the participants of the
605 individual HRC cohorts. This research has been conducted using the UK Biobank
606 Resource. We thank the Keller and Vrieze lab groups, the Institute for Behavioral
607 Genetics, and Sean Caron. This study was funded by NIH R01MH100141 (MCK),
608 NHMRC grants 1078037 (PMV) and 1113400 (PMV and JY), and Sylvia & Charles
609 Viertel Charitable Foundation Senior Medical Research Fellowship (JY).

610

611 **Haplotype Reference Consortium:** <http://www.haplotype-reference-consortium.org/>
612 Gonçalo Abecasis, David Altshuler, Carl A Anderson, Andrea Angius, Jeffrey C Barrett, Sonja
613 Berndt, Michael Boehnke, Dorrett Boomsma, Kari Branham, Gerome Breen, Chad M Brummett,
614 Fabio Busonero, Harry Campbell, Peter Campbell, Andrew Chan, Sai Chen, Emily Chew,
615 Massimiliano Cocca, Francis S Collins, Laura J Corbin, Francesco Cucca, Petr Danecek,
616 Sayantan Das, Paul I W de Bakker, George Dedoussis, Annelot Dekker, Olivier Delaneau,
617 Marcus Dorr, Richard Durbin, Aliko-Eleni Farmaki, Luigi Ferrucci, Lukas Forer, Ross M Fraser,
618 Timothy Frayling, Christian Fuchsberger, Stacey Gabriel, Ilaria Gandin, Paolo Gasparini,
619 Christopher E Gillies, Arthur Gilly, Leif Groop, Tabitha Harrison, Andrew Hattersley, Oddgeir L
620 Holmen, Kristian Hveem, William Iacono, Amit Joshi, Hyun Min Kang, Hamed Khalili, Charles
621 Kooperberg, Seppo Koskinen, Matthias Kretzler, Warren Kretzschmar, Alan Kwong, James C
622 Lee, Shawn Levy, Yang Luo, Anubha Mahajan, Jonathan Marchini, Steven McCarroll, Mark I
623 McCarthy, Shane McCarthy, Matt McGue, Melvin McInnis, Thomas Meitinger, David Melzer,
624 Massimo Mezzavilla, Josine L Min, Karen L Mohlke, Richard M Myers, Matthias Nauck,
625 Deborah Nickerson, Aarno Palotie, Carlos Pato, Michele Pato, Ulrike Peters, Nicola Pirastu,
626 Wouter Van Rheenen, J Brent Richards, Samuli Ripatti, Cinzia Sala, Veikko Salomaa, Matthew
627 G Sampson, David Schlessinger, Robert E Schoen, Sebastian Schoenherr, Laura J Scott, Kevin
628 Sharp, Carlo Sidore, P Eline Slagboom, Kerrin Small, George Davey Smith, Nicole Soranzo,
629 Timothy Spector, Dwight Stambolian, Anand Swaroop, Morris A Swertz, Alexander Teumer,
630 Nicholas Timpson, Daniela Toniolo, Michela Traglia, Marcus Tuke, Jaakko Tuomilehto, Leonard
631 H Van den Berg, Cornelia M van Duijn, Jan Veldink, John B Vincent, Uwe Volker, Scott Vrieze,
632 Klaudia Walter, Cisca Wijmenga, Cristen Willer, James F Wilson, Andrew R Wood, Eleftheria
633 Zeggini, He Zhang

634

635

636 **WHI Acknowledgment:**

637 *The WHI program is funded by the National Heart, Lung, and Blood Institute, National Institutes*
638 *of Health, U.S. Department of Health and Human Services through contracts*
639 *HHSN268201600018C, HHSN268201600001C, HHSN268201600002C, HHSN268201600003C,*
640 *and HHSN268201600004C. The authors thank the WHI investigators and staff for their*
641 *dedication, and the study participants for making the program possible. A full listing of WHI*
642 *investigators can be found at:*
643 [http://www.whi.org/researchers/Documents%20%20Write%20a%20Paper/WHI%20Investigator](http://www.whi.org/researchers/Documents%20%20Write%20a%20Paper/WHI%20Investigator%20Long%20List.pdf)
644 [%20Long%20List.pdf](http://www.whi.org/researchers/Documents%20%20Write%20a%20Paper/WHI%20Investigator%20Long%20List.pdf)
645
646

647 **CONFLICT OF INTEREST:** The authors declare no conflicts of interest.

648 **DATA ARCHIVING:** Data are from the Haplotype Reference Consortium and the UK
649 Biobank and can be accessed through those resources.

650

651 **REFERENCES**

652 Bhatia G, Gusev A, Loh P-R, Finucane HK, Vilhjalmsdottir BJ, Ripke S, *et al.* (2016).

653 Subtle stratification confounds estimates of heritability from rare variants. *bioRxiv:*
654 048181.

655 Bjelland DW, Lingala U, Patel P, Jones M, Keller MC (2017). A fast and accurate
656 method for detection of IBD shared haplotypes in genome-wide SNP data. *Eur J*
657 *Hum Genet* **25**: 617–624.

658 Browning SR, Browning BL (2013). Identity-by-descent-based heritability analysis in the
659 Northern Finland Birth Cohort. *Hum Genet* **132**: 129–138.

660 Bulik-Sullivan BK, Loh P-R, Finucane HK, Ripke S, Yang J, Consortium SWG of the
661 PG, *et al.* (2015). LD Score regression distinguishes confounding from polygenicity
662 in genome-wide association studies. *Nat Genet* **47**: 291–295.

663 Burnham KP, Anderson DR (2002). *Model Selection and Multi-Model Inference*, Second
664 Edn. Springer New York.

- 665 Chang CC, Chow CC, Tellier LC, Vattikuti S, Purcell SM, Lee JJ, *et al.* (2015). Second-
666 generation PLINK: rising to the challenge of larger and richer datasets. *Gigascience*
667 **4**: 7.
- 668 Coventry WL, Keller MC (2005). Estimating the Extent of Parameter Bias in the
669 Classical Twin Design : A Comparison of Parameter Estimates From Extended
670 Twin-Family and Classical Twin Designs. **8**: 214–223.
- 671 Das S, Forer L, Schönherr S, Sidore C, Locke AE, Kwong A, *et al.* (2016). Next-
672 generation genotype imputation service and methods. *Nat Genet* **48**: 1284–1287.
- 673 Delaneau O, Zagury J-F, Marchini J (2013). Improved whole-chromosome phasing for
674 disease and population genetic studies. *Nat Methods* **10**: 5–6.
- 675 Eaves LJ, Last KA, Young PA, Martin NG (1978). Model-fitting approaches to the
676 analysis of human behaviour. *Heredity* **41**: 249–320.
- 677 Evans LM, Tahmasbi R, Vrieze SI, Abecasis GR, Das S, Bjelland DW, *et al.* (2017).
678 Comparison of methods that use whole genome data to estimate the heritability
679 and genetic architecture of complex traits. *bioRxiv*: 115527.
- 680 Falconer DS, Mackay TFC (1996). *Introduction to Quantitative Genetics*, Longman
681 Limited: Harlow, Essex, England.
- 682 Gusev A, Lowe JK, Stoffel M, Daly MJ, Altshuler D, Breslow JL, *et al.* (2009). Whole
683 population, genome-wide mapping of hidden relatedness. *Genome Res* **19**: 318–
684 326.
- 685 Hayes BJ, Visscher PM, Goddard ME (2009). Increased accuracy of artificial selection
686 by using the realized relationship matrix. *Genet Res (Camb)* **91**: 47–60.
- 687 Keller MC, Coventry WL (2005). Quantifying and addressing parameter indeterminacy

688 in the classical twin design. *Twin Res Hum Genet* **8**: 201–213.

689 Lee SH, DeCandia TR, Ripke S, Yang J, Sullivan PF, Goddard ME, *et al.* (2012).
690 Estimating the proportion of variation in susceptibility to schizophrenia captured by
691 common SNPs. *Nat Genet* **44**: 247–250.

692 Locke AE, Kahali B, Berndt SI, Justice AE, Pers TH, Day FR, *et al.* (2015). Genetic
693 studies of body mass index yield new insights for obesity biology. *Nature* **518**: 197–
694 206.

695 Lynch M, Walsh B (1998). *Genetics and Analysis of Quantitative Traits*. Sinauer
696 Associates: Sunderland, MA.

697 Martin NG, Eaves LJ, Kearsley MJ, Davies P (1978). The power of the classical twin
698 study. *Heredity* **40**: 97–116.

699 Mathieson I, McVean G (2012). Differential confounding of rare and common variants in
700 spatially structured populations. *Nat Genet* **44**: 243–6.

701 McCarthy S, Das S, Kretzschmar W, Delaneau O, Wood AR, Teumer A, *et al.* (2016). A
702 reference panel of 64,976 haplotypes for genotype imputation. *Nat Genet* **48**:
703 1279–1283.

704 Polderman TJC, Benyamin B, de Leeuw CA, Sullivan PF, van Bochoven A, Visscher
705 PM, *et al.* (2015). Meta-analysis of the heritability of human traits based on fifty
706 years of twin studies. *Nat Genet* **47**: 702–709.

707 Price AL, Helgason A, Thorleifsson G, McCarroll SA, Kong A, Stefansson K (2011).
708 Single-tissue and cross-tissue heritability of gene expression via identity-by-
709 descent in related or unrelated individuals. *PLoS Genet* **7**.

710 Price AL, Zaitlen N a, Reich D, Patterson N (2010). New approaches to population

711 stratification in genome-wide association studies. *Nat Rev Genet* **11**: 459–63.

712 Ripke S, Neale BM, Corvin A, Walters JTR, Farh K-H, Holmans PA, *et al.* (2014).

713 Biological insights from 108 schizophrenia-associated genetic loci. *Nature* **511**:

714 421–427.

715 Robinson MR, Hemani G, Medina-Gomez C, Mezzavilla M, Esko T, Shakhbazov K, *et*

716 *al.* (2015). Population genetic differentiation of height and body mass index across

717 Europe. *Nat Genet* **47**: 1357–1362.

718 Speed D, Hemani G, Johnson MR, Balding DJ (2012). Improved heritability estimation

719 from genome-wide SNPs. *Am J Hum Genet* **91**: 1011–1021.

720 Sudlow C, Gallacher J, Allen N, Beral V, Burton P, Danesh J, *et al.* (2015). UK Biobank:

721 An Open Access Resource for Identifying the Causes of a Wide Range of Complex

722 Diseases of Middle and Old Age. *PLoS Med* **12**: 1–10.

723 Tenesa A, Haley CS (2013). The heritability of human disease: estimation, uses and

724 abuses. *Nat Rev Genet* **14**: 139–149.

725 Visscher PM, Brown MA, McCarthy MI, Yang J (2012). Five years of GWAS discovery.

726 *Am J Hum Genet* **90**: 7–24.

727 Visscher PM, Hill WG, Wray NR (2008). Heritability in the genomics era - concepts and

728 misconceptions. *Nat Genet* **9**: 255–266.

729 Visscher PM, Medland SE, Ferreira M a R, Morley KI, Zhu G, Cornes BK, *et al.* (2006).

730 Assumption-free estimation of heritability from genome-wide identity-by-descent

731 sharing between full siblings. *PLoS Genet* **2**: e41.

732 Wakeley J (2009). *Coalescent Theory: An Introduction*. Roberts and Company:

733 Greenwood Village, CO.

734 Wood AR, Esko T, Yang J, Vedantam S, Pers TH, Gustafsson S, *et al.* (2014). Defining
735 the role of common variation in the genomic and biological architecture of adult
736 human height. *Nat Genet* **46**: 1173–86.

737 Yang J, Bakshi A, Zhu Z, Hemani G, Vinkhuyzen AAE, Lee SH, *et al.* (2015). Genetic
738 variance estimation with imputed variants finds negligible missing heritability for
739 human height and body mass index. *Nat Genet* **47**: 1114–20.

740 Yang J, Benyamin B, McEvoy BP, Gordon S, Henders AK, Nyholt DR, *et al.* (2010).
741 Common SNPs explain a large proportion of the heritability for human height. *Nat*
742 *Genet* **42**: 565–569.

743 Yang J, Lee SH, Goddard ME, Visscher PM (2011). GCTA: A tool for genome-wide
744 complex trait analysis. *Am J Hum Genet* **88**: 76–82.

745 Yang J, Manolio TA, Pasquale LR, Boerwinkle E, Caporaso N, Cunningham JM, *et al.*
746 (2011). Genome partitioning of genetic variation for complex traits using common
747 SNPs. *Nat Genet* **43**: 519–25.

748 Zaitlen N, Kraft P, Patterson N, Pasaniuc B, Bhatia G, Pollack S, *et al.* (2013). Using
749 extended genealogy to estimate components of heritability for 23 quantitative and
750 dichotomous traits. *PLoS Genet* **9**.

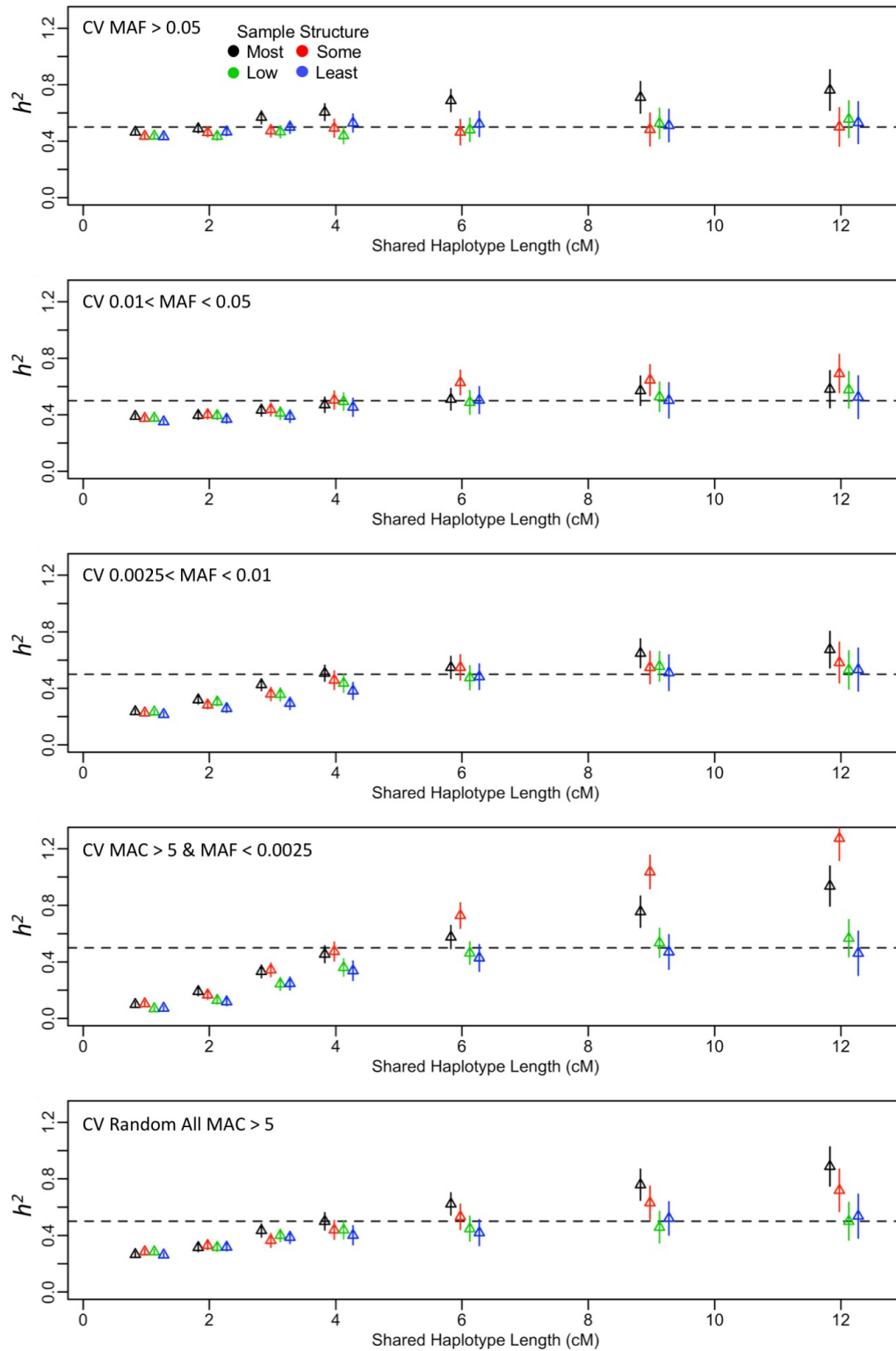
751 Zuk O, Hechter E, Sunyaev SR, Lander ES (2012). The mystery of missing heritability:
752 Genetic interactions create phantom heritability. *Proc Natl Acad Sci U S A* **109**:
753 1193–8.

754

755

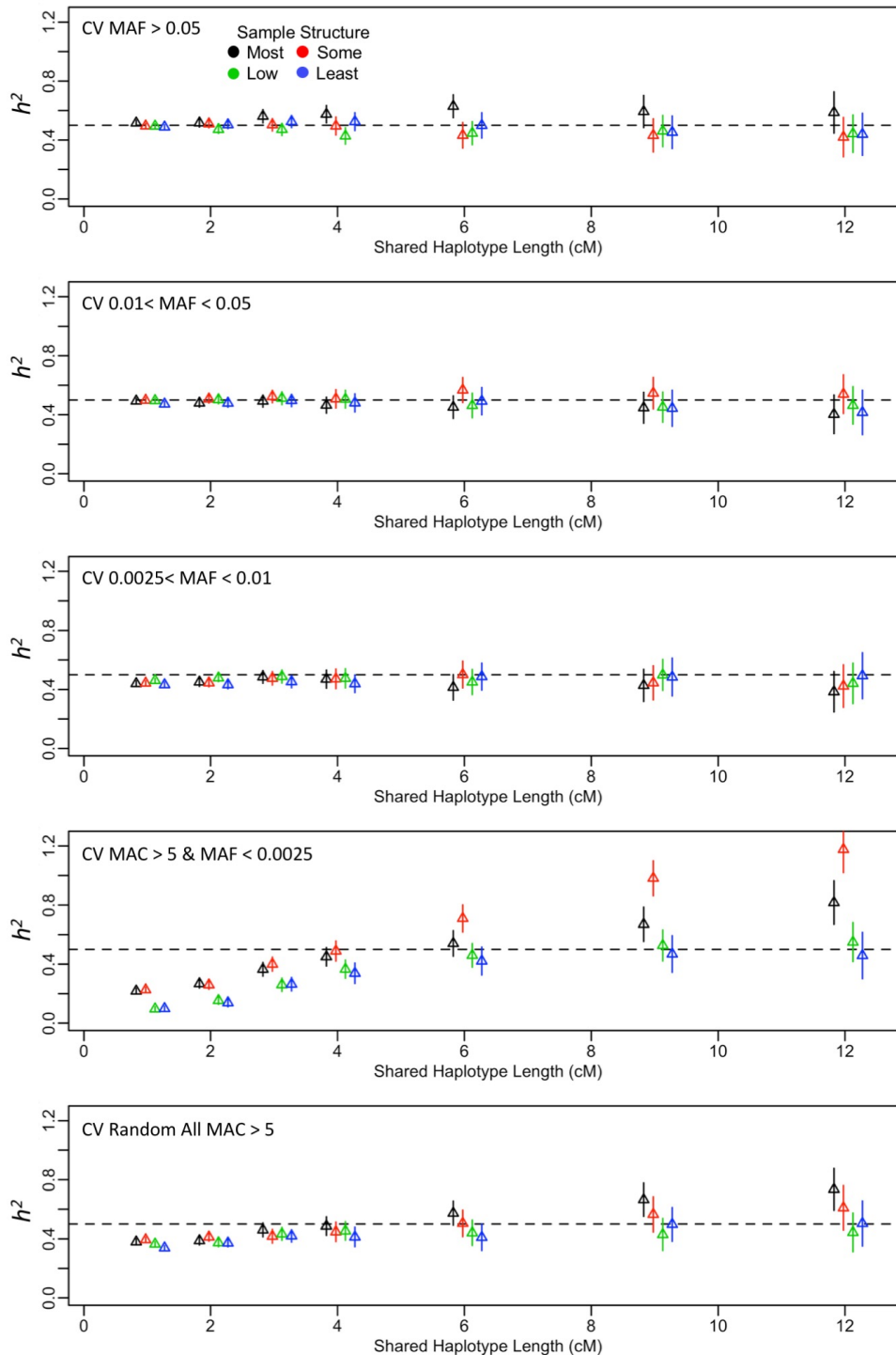
756

757 **FIGURE LEGENDS**



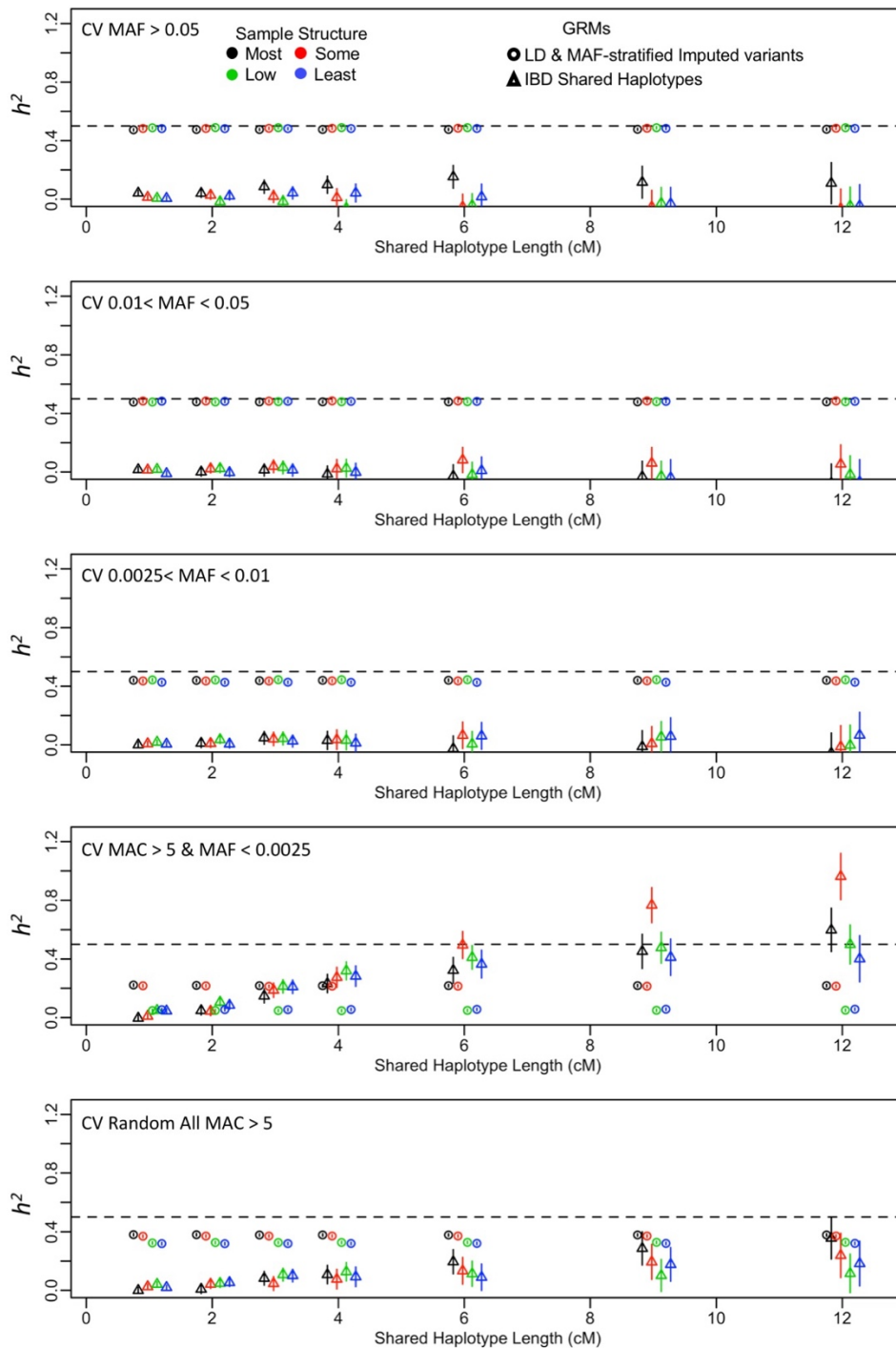
758 **Figure 1.** GREML-SC using an IBD-GRM. h^2_{IBD} estimates (mean \pm 95% CI from 400
759 replicates). X axis indicates the IBD shared haplotype length threshold for the IBD-
760 GRM. Phenotypes with 1,000 CVs randomly drawn from the MAF range specified in
761

762 each panel. Different colors indicate degree of stratification in the sample. Relatedness
763 cutoff of 0.05 used.



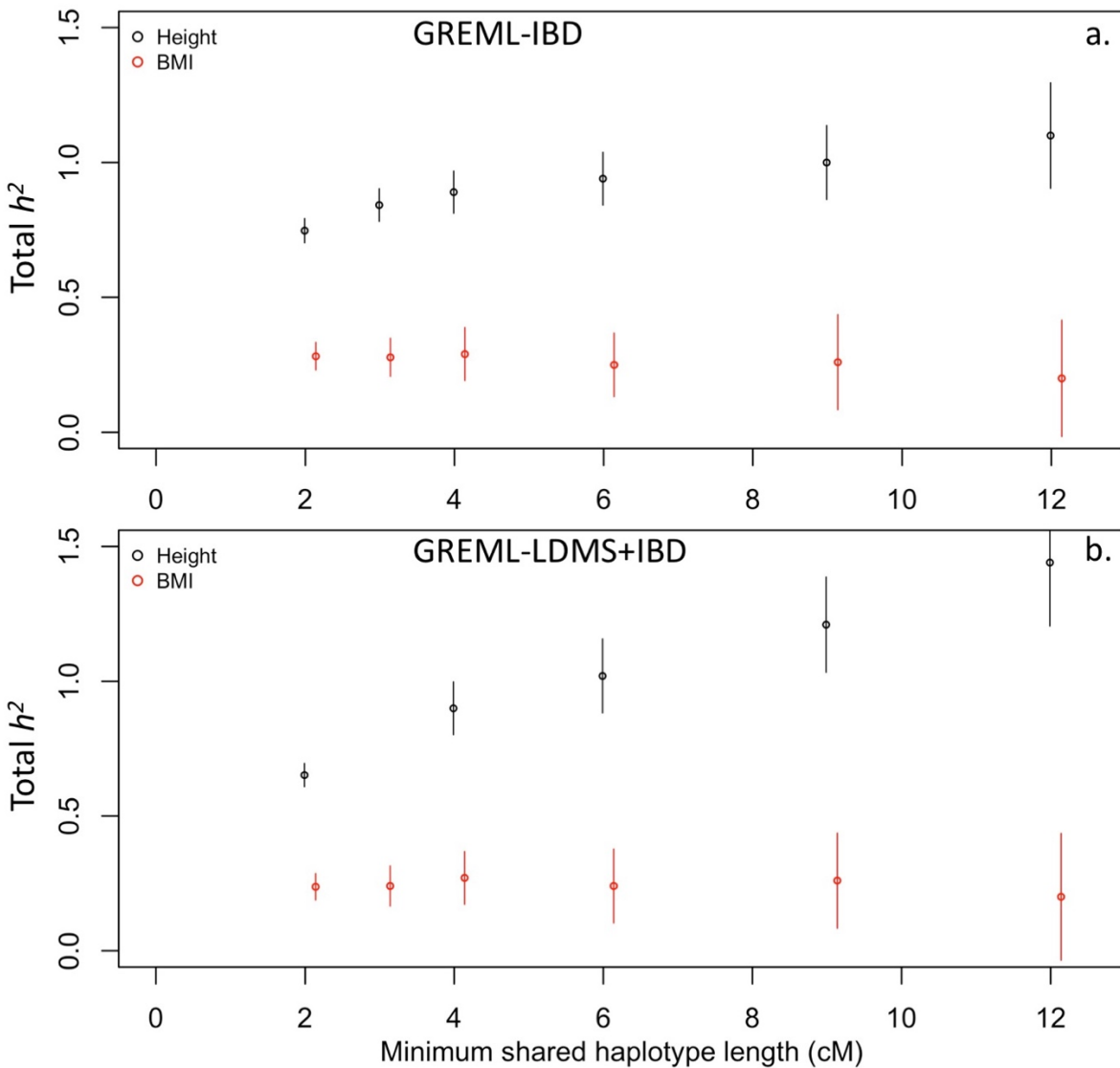
764
765 **Figure 2.** GREML-LDMS+IBD model. This model had 13 components, 12 LD & MAF-
766 stratified GRMs using imputed genome-wide variants, and one GRM from IBD shared
767 haplotypes. Total h^2 estimates are shown (mean \pm 95% CI from 400 replicates). X axis
768 indicates the different IBD shared haplotype length thresholds for the IBD-GRM.
769 Phenotypes with 1,000 CVs randomly drawn from the MAF range specified in each

770 panel. Different colors indicate degree of stratification in the sample. Relatedness cutoff
 771 of 0.05 used.



772
 773 **Figure 3.** GREML-LDMS+IBD. This model had 13 components, 12 LD & MAF-stratified
 774 GRMs using imputed genome-wide variants, and one GRM from IBD shared
 775 haplotypes. Separate h^2 estimates for each component are given by the symbols (mean
 776 \pm 95% CI from 400 replicates). Note that the “Imputed LDMS” symbol represents the
 777 sum of the imputed LDMS GRM variance estimates. X axis indicates the different IBD
 778 shared haplotype length thresholds for the IBD-GRM. Phenotypes with 1,000 CVs

779 randomly drawn from the MAF range specified in each panel. Different colors indicate
780 degree of stratification in the sample. Relatedness cutoff of 0.05 used.



781
782 **Figure 4.** Total heritability estimates for three continuous traits in the UK Biobank. (a)
783 GREML-IBD, which had a single IBD-GRM. (b) GREML-LDMS+IBD for three
784 continuous traits in the UK Biobank. This model had 13 components, 12 LD & MAF-
785 stratified GRMs using imputed genome-wide variants, and one GRM from IBD shared
786 haplotypes. Total h^2 estimates are shown (\pm 95% CI). X axis indicates the different IBD
787 shared haplotype length thresholds for the IBD-GRM. Relatedness cutoff of 0.05 used.
788